STEM CELLS AND DEVELOPMENT
Volume 23, Number 22, 2014

DOI: 10.1089/scd.2013.0630

Reversible Mitochondrial DNA Accumulation in Nuclei of Pluripotent Stem Cells

Joel S. Schneider,[1,*] Xin Cheng,[1,*] Qingshi Zhao,[1,*] Chingiz Underbayev,[2,*] J. Patrick Gonzalez,[1,*] Elizabeth S. Raveche,[2] Diego Fraidenraich,[1] and Andreas S. Ivessa[1]

According to the endosymbiotic hypothesis, the precursor of mitochondria invaded the precursor of eukaryotic cells, a process that began roughly 2 billion years ago. Since then, the majority of the genetic material translocated from the mitochondria to the nucleus, where now almost all mitochondrial proteins are expressed. Only a tiny amount of DNA remained in the mitochondria, known as mitochondrial DNA (mtDNA). In this study, we report that the transfer of mtDNA fragments to the nucleus of pluripotent stem cells is still ongoing. We show by in situ hybridization and agarose DNA two-dimensional gel technique that induced pluripotent stem (iPS) cells contain high levels of mtDNA in the nucleus. We found that a large proportion of the accumulated mtDNA sequences appear to be extrachromosomal. Accumulation of mtDNA in the nucleus is present not only in the iPS cells, but also in embryonic stem (ES) cells. However upon differentiation, the level of mtDNA in the nuclei of iPS and ES cells is substantially reduced. This reversible accumulation of mtDNA in the nucleus supports the notion that the nuclear copy number of mtDNA sequences may provide a novel mechanism by which chromosomal DNA is dynamically regulated in pluripotent stem cells.

Introduction

Nuclear DNA sequences of mitochondrial origin (NUMTs) are believed to act as molecular fossils, which indicate the evolutionary flow of genetic information from the mitochondria to the nucleus [1]. However, a few yeast studies demonstrate that this flow of genetic information is still ongoing. For example, plasmid DNA, which can be maintained in both the mitochondria and the nucleus, can translocate from the mitochondria to the nucleus, but is not believed to migrate in the opposite direction [2]. Further, mitochondrial DNA (mtDNA) fragments can be captured during the repair of induced double-stranded (ds) DNA breaks in yeast chromosomes [3–6]. There are also some reports that de novo disruptions of specific nuclear genes by mtDNA insertions are likely implicated in the initiation of a few human diseases [1,7–12]. For example, the de novo disruption of the human *GLI3* gene by a short mtDNA fragment was able to induce Pallister-Hall syndrome in a patient [7]. mtDNA was also detected in the nucleus of tumor cells (eg, gliomas), however, the significance of nuclear-localized mtDNA in tumorigenesis is unknown [13,14]. The rate of mtDNA fragments migrating to the nucleus increases during aging in both yeast and mammals suggesting that mtDNA fragments in the nucleus affect aging [15–17].

Although the method of reprogramming somatic cells to induced pluripotent stem (iPS) cells by using the SKOM factors (ie, Sox2, Klf4, Oct3/4, c-Myc) is very convenient, most somatic cells expressing these factors fail to complete reprogramming and remain as precursors of stem cells, which often undergo apoptosis, senescence or cell cycle arrest [18–20]. Many current reprogramming methods have low efficiencies [18,19,21–23]. Although various reasons for the low reprogramming efficiency have been discussed [20,21], one possibility is that frequent nuclear DNA damage during reprogramming lowers the reprogramming efficiency [20,21,24–41]. The effect of the oncogenes c-Myc and Klf4 may contribute to this observation [42,43]. Despite these significant changes in the genomic DNA, nuclear trafficking and/or amplification of mtDNA has never been considered as a potential player in the process of reprogramming.

We wanted to test the hypothesis that during reprogramming, fragments of mtDNA migrate to the nucleus and accumulate, which may eventually affect nuclear genomic stability and reprogramming efficiency. In this study, we demonstrate that pluripotent stem cells contain amplified mtDNA sequences in their nuclei, mainly in an extrachromosomal form, and that this accumulation is reversible in pluripotent stem cells subjected to differentiation.

[1]Department of Cell Biology and Molecular Medicine and [2]Department of Pathology, Rutgers New Jersey Medical School, Rutgers Biomedical and Health Sciences, Newark, New Jersey.
*These authors contributed equally to this work.

Materials and Methods

Cell lines, generation of iPS cells, differentiation of pluripotent stem cells

Two and three independent mouse iPS and embryonic stem (ES) cell lines were used, respectively. We used mouse embryonic fibroblasts (MEFs) derived from C57BL/10 mice for reprogramming. This iPS cell line was generated by expressing Sox2, Klf4, and Oct3/4 (SKO factors) on a single plasmid, which was then introduced into fibroblasts by lentivirus transduction [44]. Expression of c-Myc was omitted in this cell line. iPS cell colonies were identified essentially as previously described by the Yamanaka laboratory [18,19]. The second iPS cell line was originally generated by expressing all four reprogramming factors Sox2, Klf4, Oct3/4, and c-Myc (SKOM factors) individually on plasmids, which were introduced into MEFs by retrovirus transduction (generously provided by Dr. Rudolf Jaenisch, Whitehead Institute, Cambridge) [45]. This iPS cell line expresses a GFP gene driven by the Oct4-promoter. The MEFs were passaged three times and the iPS cells about 15 times before analysis. The Rosa 26 ES cell line, which was generously provided by Dr. Philippe Soriano at the Mount Sinai School of Medicine, NY, was passaged multiple times (Fig. 3) [46]. A second cell line (MUBES-01201; Cyagen Biosciences), which was passaged 25 times, expressed a red fluorescent protein (Supplementary Fig. S5; Supplementary Data are available online at www.liebertpub.com/scd) and a third ES cell line, which was passaged about ten times, which was generously provided by Dr. Eun Jung Lee, NJIT, NJ, expressed a GFP reporter under the cardiac troponin T promoter (Fig. 4). Induction of differentiation to iPS and ES cells was carried out according to the hanging drop method as described by Dr. Elizabeth Lacy's lab at Memorial Sloan Kettering Cancer Center, NY [47]. Overall, the passage number did not appear to affect the amount of nuclear mtDNA in the pluripotent stem cells. mtDNA was depleted from mitochondria by growing the iPS cells (reprogrammed using the SKO factors) for 24 h in a medium containing 500 ng/mL ethidium bromide and supplemented with uridine and pyruvate [48,49].

Fluorescence in situ hybridization

To visualize mtDNA in mammalian cells, we applied a protocol for fluorescence in situ hybridization (FISH) similar to one described in Caro et al. [17]. In some experiments mitochondria were labeled with the live cell stain MitoTracker Red® (Invitrogen) before fixation of the cells in 4% paraformaldehyde. Cells were permeabilized with 0.2% Triton X-100 for 20 min at room temperature (RT) and RNA was digested using 1 μg/mL RNaseA for 1 h at 37°C. Cells were blocked (prehybridization) with 4% bovine serum albumin (BSA) for 1 h and then dehydrated in 70%, 90%, and 100% ethanol. The hybridization solution consisted of 70% deionized formamide (Sigma), 12 mM Tris-HCl (pH 8), 5 mM KCl, 1 mM $MgCl_2$, 0.001% Triton X-100, and 0.25% acetylated BSA (Sigma). Cells attached to a coverslip were put upside down on a slide having a drop (25 μL) of hybridization liquid containing the labeled DNA probes at an approximate concentration of 2 ng/mL. DNA was denatured by putting the slide on a heat block (80°C) for 5 min followed by cooling down on the bench. The hybridization was continued in a moist chamber at RT overnight. The cells on the coverslips were washed with 70% formamide and 2× SSC four times for 10 min each, and then covered with the mounting medium containing DAPI (Fluoroshield™; Sigma). Cells were analyzed using an epifluorescence microscope (Nikon Eclipse 80i) equipped with a CCD camera (DS-Qi1).

DNA two-dimensional gel electrophoresis

We purified nuclear and mtDNA as previously described [50]. We used the mild detergent NP-40 to remove mtDNA molecules, which are present in mitochondria attached to the purified nuclei. Nuclear and mtDNA were then analyzed by two-dimensional (2D) agarose gel electrophoresis technique as previously applied [51]. DNA samples were separated on a 0.31% agarose gel for 24 h at 1 V/cm in the first dimension and on a 0.8% agarose gel for 48 h at 1.5 V/cm in the second dimension. Both agarose gels contained 0.5 μg/mL ethidium bromide. The 2D gel membranes were hybridized to a ^{32}P-labeled mtDNA probe containing fragments #1 to #5 (see below).

Sequences of primers used in PCR and in preparing the DNA probes

mtDNA fragment #1 (12S rRNA) (Primer 69 F mouse mtDNA: 5′-CAAAGGTTTGGTCCTGGCCT; primer 790 R mouse mtDNA: 5′-TGTAGCCCATTTCTTCCCA)

mtDNA fragment #2 (16S rRNA) (Primer 2100 F mouse mtDNA: 5′-CTTTAATCAGTGAAATTGACCTTTCAG; primer 2650 R mouse mtDNA: 5′-CGTATATATTTTATT TAGATTTTATTCATAAATTAAG)

mtDNA fragment #3 (Cox1) (Primer 5215 F mouse mtDNA: 5′-CACCTTCGAATTTGCATTCG; primer 5709 R mouse mtDNA: 5′-CTGTTCATCCTGTTCCTGCT)

mtDNA fragment #4 (ATPase 6) (Primer 8032 F mouse mtDNA: 5′-CGCCTAATCAACAACCGTCT; primer 8497 R mouse mtDNA: 5′-TGGTAGCTGTTGGTGGGCTA)

mtDNA fragment #5 (ND5) (Primer 12777 F mouse mtDNA: 5′-CATAGCCTGGCAGACGAACA; primer 13435 R mouse mtDNA: 5′-GAGGTGGATTTTGGGATGGT)

DNA fragment GAPDH (Primer 135961 mouse GAPDH-F: 5′-ATCACGCCACAGCTTTCCAGAG; primer 136700 mouse GAPDH-R: 5′-GCAAAGTGGAGATTGTTGCCA TCAA)

To amplify the ~12 kb mtDNA fragment we used the Takara LA Taq® polymerase and primers 12777 F mouse mtDNA and 8497 R mouse mtDNA (see above for the sequence).

Cy3-labeled PNA mammalian telomere probe (generously provided by Dr. Utz Herbig, Rutgers Biomedical and Health Sciences, Newark).

For the FISH PCR-generated DNA fragments were labeled directly with Alexa Fluor® 488 or Alexa Fluor® 546 using the ULYSIS® nucleic acid labeling kit (Molecular Probes).

The PCR fragments amplified from nuclear MEF and iPS cell genomic DNA were sequenced at the company Macrogen USA Corp. For the sequence alignment we used BLASTN (Basic Local Alignment Search Tool).

Statistical analysis

We repeated each experiment at least three times and we used the Student's *t*-test to calculate *P* values.

Results and Discussion

The number of mtDNA sequences with nuclear localization, which were visualized by FISH, increase during aging in rat liver and brain [17]. Given that mtDNA fragments may translocate from mitochondria to the nucleus and potentially disrupt specific nuclear genes by insertion mutagenesis, we investigated whether mtDNA fragments also accumulate in the nucleus during reprogramming [1]. We used the same FISH protocol that was used to detect mtDNA insertions in nuclear DNA of brain and liver tissues of rats [17]. The mtDNA probes were amplified by PCR using mtDNA purified from cardiac mouse mitochondria, and labeled by covalently linking fluorophores (see Materials and Methods section). All five mtDNA probes (#1– #5) together were used in the hybridization experiments. General cellular DNA was stained with DAPI, and the mitochondria were visualized using the dye MitoTracker Red (Invitrogen) before fixation of the cells with formaldehyde.

We used mouse embryonic fibroblasts (MEFs) and iPS cells derived from MEF cells expressing the three reprogramming factors Sox2, Klf4, and Oct3/4 (SKO) [19,52]. In fibroblasts, the cytosolic mtDNA signals, which were likely derived from mtDNA within the mitochondria, were hazy most likely because the cells were treated with RNase before hybridization (Fig. 1A and Supplementary Fig. S1). Several discrete signals indicating mtDNA-like sequences were observed in the nucleus, which colocalized with the nuclear

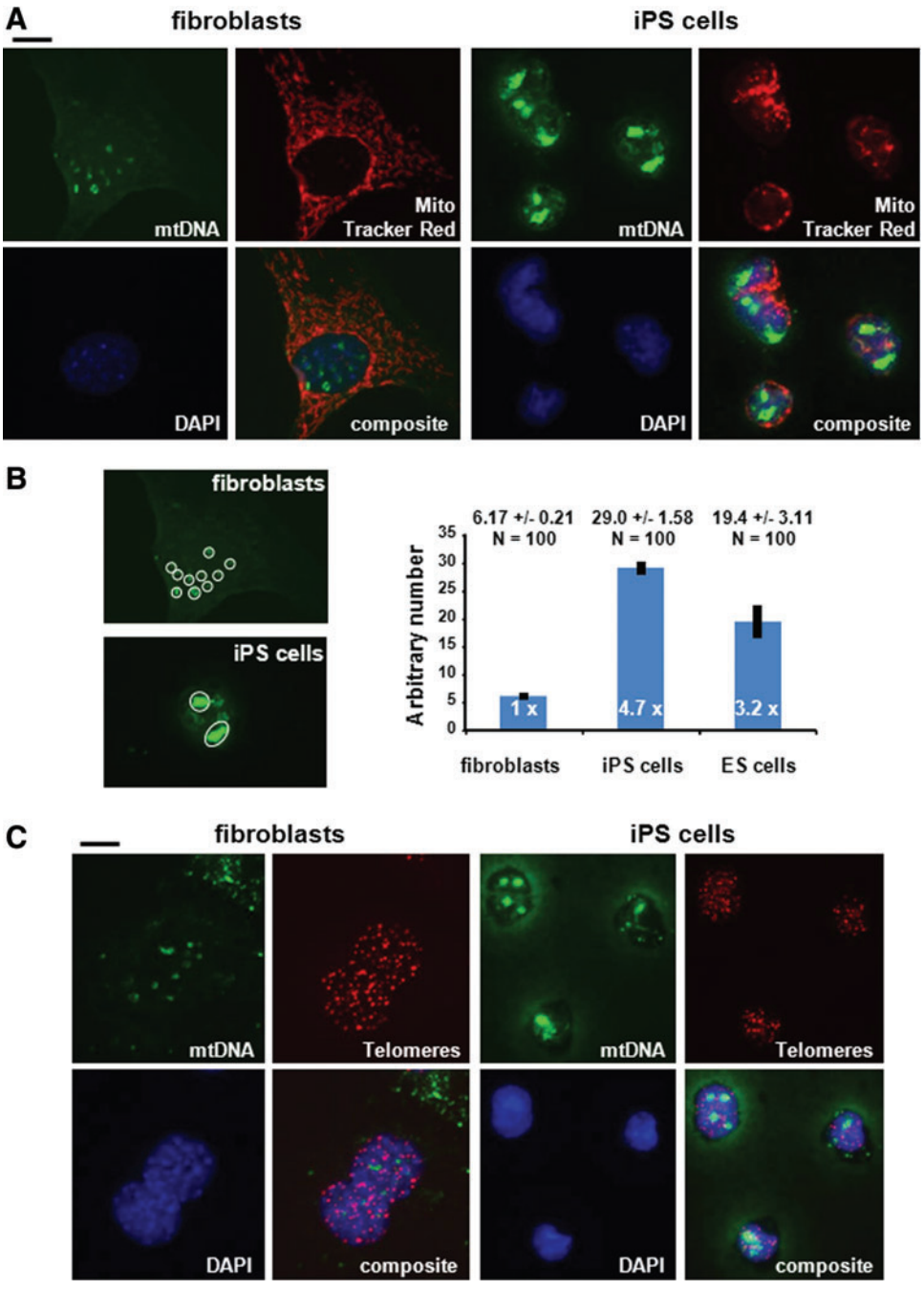

FIG. 1. mtDNA sequences accumulate in the nucleus of iPS cells. **(A)** MEFs and iPS cells (reprogrammed by using the SKO factors) were processed for in situ hybridization. Nuclear staining for mtDNA superimposes with nuclear DAPI staining. *Green:* mtDNA (Alexa Fluor® 488-labeled mtDNA fragments); *blue:* DNA (DAPI); *red:* mitochondria (MitoTracker Red). A low exposure for DAPI was chosen, therefore mtDNA in the cytoplasm is not visible. The staining of mtDNA in the cytoplasm is very light because the cells were treated with RNase before the hybridization (see Materials and Methods section). Scale bar: 5 μm. **(B)** The intensities of the mtDNA staining in the nucleus of MEFs, iPS, and ES (see Fig. 3) cells in the immunofluorescence images were determined using the program ImageJ and expressed as arbitrary numbers. Standard errors are displayed regarding the indicated number of analyzed cells. **(C)** Colocalization of mtDNA and telomere sequences in MEFs and iPS cells. *Green:* mtDNA (Alexa Fluor 488-labeled mtDNA fragments); *red:* telomere DNA (Cy3-labeled telomere DNA); *blue:* DNA (DAPI). Scale bar: 5 μm. ES, embryonic stem; MEFs, mouse embryonic fibroblasts; mtDNA, mitochondrial DNA. Color images available online at www.liebertpub.com/scd

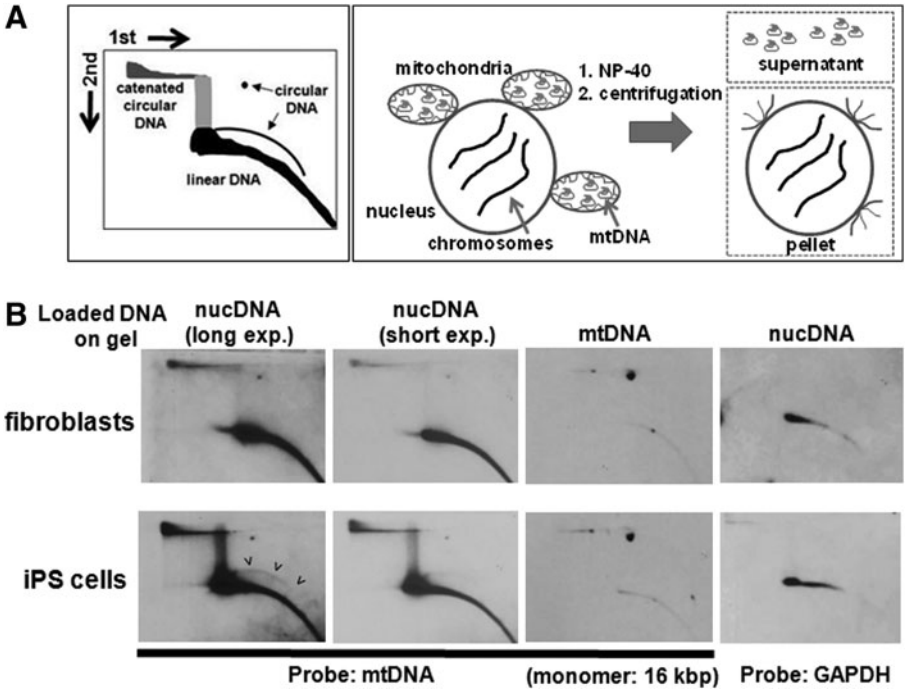

FIG. 2. The accumulation of nuclear mtDNA sequences in iPS cells is mainly of extrachromosomal nature. **(A)** *Left side:* scheme of the 2D neutral–neutral agarose gel electrophoresis and interpretation of the visualized DNA structures using Southern technique. *Right side:* scheme of the purification of nuclear and mtDNA. **(B)** Analysis of nuclear and mtDNA derived from MEFs and iPS cells (reprogrammed by using the SKO factors) by 2D agarose gel electrophoresis. The membranes were probed with a radioactive-labeled mtDNA probe. The membranes with the separated nuclear DNA were reprobed with a radioactive-labeled nuclear DNA probe (ie, *GAPDH*). 2D, two-dimensional.

DAPI staining and looked also similar as previously described by Caro et al. [17]. The amount of mtDNA in the nucleus was clearly elevated in iPS cells as determined by densitometric scanning of the fluorescence images using the program NIH ImageJ. Similar results were obtained with iPS cells derived from MEFs expressing all four reprogramming factors Sox2, Klf4, Oct3/4, and c-Myc (SKOM) (Supplementary Fig. S2) [19,52]. Although there were only one or two strong focal sites visible in iPS cells instead of several spots in fibroblasts, measurements of the intensities of the nuclear signals derived from the mtDNA-Alexa Fluor 488 stained regions demonstrated that iPS cells (SKO, Fig. 1A) contain $\sim$4.7-fold ($P < 0.005$) more mtDNA with nuclear localization compared to fibroblasts (Fig. 1B). The nuclear mtDNA signals in both fibroblasts and iPS cells appeared to occupy rather large areas in the nucleus compared to single chromosomal sequences. For comparison, we detected mtDNA and telomeric sequences in the same cells (Fig. 1C). Normal diploid mouse cells contain 40 chromosomes which equals to 80 telomeric signals. Telomeric sequence was detected with a Cy3-labeled telomere probe; mtDNA was visualized using Alexa Fluor 488-labeled mtDNA fragments. Given that the average length of telomeres in laboratory mice is between 50 to 100 kb, the telomere signals (Fig. 1C, red signals) were overall considerably smaller than many of the nuclear mtDNA signals (Fig. 1C, green signals). In addition, we detected the single nuclear *GAPDH* gene in fibroblasts and iPS cells using Alexa Fluor 488-labeled *GAPDH*-encoding DNA fragments. The *GAPDH*/FISH signals had comparable intensities in fibroblasts and iPS cells, but were also considerably smaller than the nuclear mtDNA signals shown in Figure 1 (Supplementary Fig. S3).

Previous analyses of genome sequences of iPS cells did not predict any de novo insertions of mtDNA fragments into

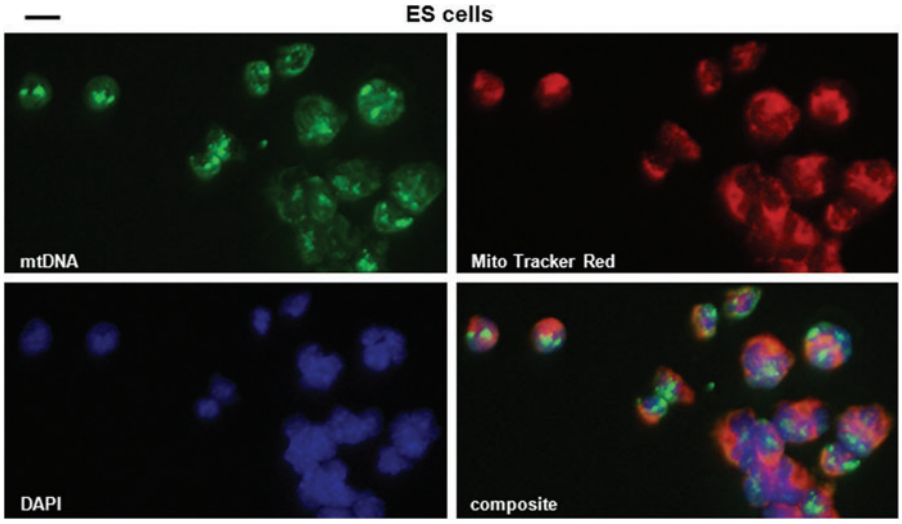

FIG. 3. mtDNA sequences accumulate in the nucleus of ES cells. Mouse ES cells (Rosa 26) were processed for in situ hybridization. Nuclear staining for mtDNA superimposes with nuclear DAPI staining. *Green:* mtDNA (Alexa Fluor 488-labeled mtDNA fragments); *blue:* DNA (DAPI); *red:* mitochondria (MitoTracker Red®). Scale bar: 5 μm. Color images available online at www.liebertpub.com/scd

nuclear DNA during reprogramming or that extensive amplification of mtDNA sequences within the chromosomal DNA sequence occurs [26,27,39,53]. To investigate whether some of the mtDNA sequences in the nucleus of iPS cells are present in extrachromosomal form, we analyzed fibroblasts and iPS cells using the 2D agarose gel electrophoresis, which allows the separation of the circular form from linear DNA molecules (Fig. 2A, cartoon in left panel) [51]. We isolated nuclei from fibroblasts and iPS cells as previously described [50]. Since crude nuclei still have some mitochondria attached to their surface, we removed the mtDNA, which is present in these mitochondria, from the nuclei by treatment with the mild detergent NP-40 (Fig. 2A, right panel). We analyzed the undigested nuclear DNA by 2D gel electrophoresis and hybridized the membrane to a radioactive-labeled mtDNA probe. The majority of the mtDNA probe is hybridizing to linear nuclear DNA of both fibroblasts and iPS cells (Fig. 2B, left four panels). We

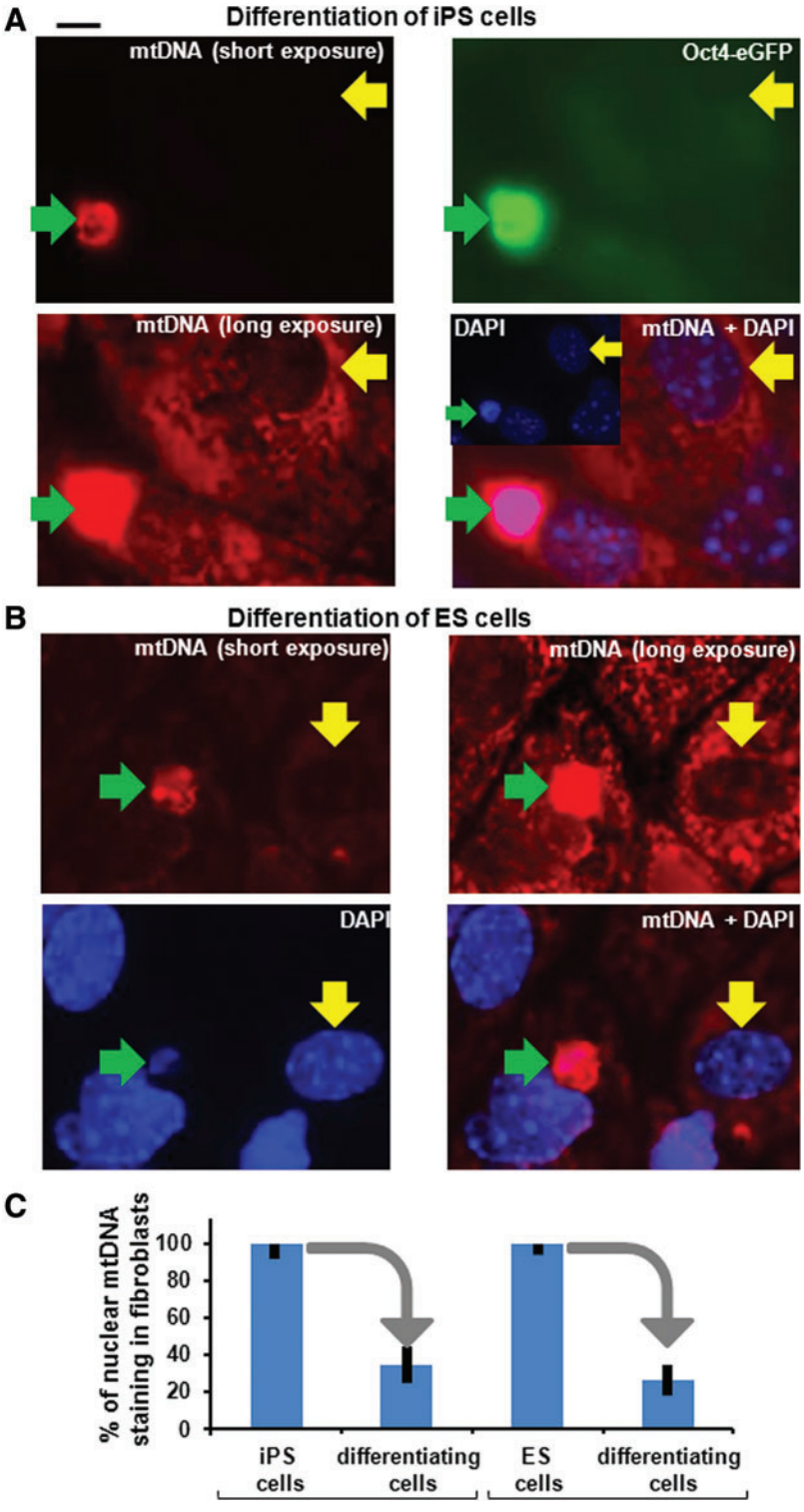

FIG. 4. The accumulation of nuclear mtDNA sequences is reversible after inducing differentiation of iPS and ES cells. **(A)** The differentiation process in iPS cells (SKOM; Oct4-eGFP) was induced using the hanging drop method. A representative image of an iPS cell with adjacent differentiating somatic cells is shown. Cells were processed for in situ hybridization. Nuclear staining for mtDNA superimposes with nuclear DAPI staining. *Green:* Oct4-eGFP; *blue:* DNA (DAPI); *red:* mtDNA (Cy3-labeled mtDNA fragments). Two different Cy3-mtDNA staining intensities are displayed in the *left two panels*. Note that the eGFP signal is lost upon differentiation. *Green arrows* indicate the pluripotent stem cell, the *yellow arrows* depict a differentiated cell. Scale bar: 5 μm. **(B)** The differentiation process in ES cells was induced using the hanging drop method. A representative image of an ES cell with adjacent differentiating somatic cells is shown. Cells were processed for in situ hybridization. Nuclear staining for mtDNA superimposes with nuclear DAPI staining. *red:* mtDNA (Cy3-labeled mtDNA fragments); *blue:* DNA (DAPI). *Green arrows* indicate the pluripotent stem cell, the *yellow arrows* depict a differentiated cell. **(C)** The intensities of the mtDNA staining in the nuclei of iPS, ES, and differentiated cells in the immunofluorescence images were determined using the program ImageJ. The intensities of the nuclear mtDNA signals were set to 100% in iPS and in ES cells. They decreased to 34% ± 15% in differentiating cells derived from iPS cells and to 26% ± 12% in differentiating cells derived from ES cells. Fifty cells each were scored. Standard errors are displayed. Color images available online at www.liebertpub.com/scd

propose that these sequences are not extrachromosomal, but are rather part of chromosomal DNA, for example in the form of NUMTs which are mtDNA sequences dispersed throughout chromosomal DNA [1]. In the nuclear DNA of iPS cells, we observed an approximate sixfold increase compared to fibroblasts (determined by phosphorimager) of a DNA species, which does not appear to enter the gel (top left side). It is possible that these molecules are mtDNA circles linked to each other in the form of concatemers as previously described [54,55]. In the iPS gel there is a further arc above the arc of linear DNA fragments, which may also indicate circular mtDNA species of various sizes. As a control, we also analyzed mtDNA derived from the mitochondrial fraction by 2D gel electrophoresis (Fig. 2B). mtDNA has a size of about 16 kb and is mainly present in circular form as a monomer in mitochondria. The full-length circular DNA appears as a homogenous DNA species (visualized as a spot) in the 2D gel, thus mtDNA in mitochondria is mainly present in monomeric, circular form. The weak signal on the arc of linear DNA fragments indicates likely contamination from nuclear DNA. The mtDNA gels also clearly indicate that the nuclear DNA samples are mostly free of full-length mtDNA molecules, which derive from mitochondria attached to the nucleus. As another control, we reprobed the nuclear DNA gels with a probe against the single-copy gene *GAPDH*. No extrachromosomal *GAPDH* DNA circles are visible in the iPS gel. To determine further, the size of the highly abundant mtDNA sequences, we amplified short (0.5–0.8 kb) and long ($\sim$12 kb) mtDNA sequences by PCR (Supplementary Fig. S4). Whereas there was an approximately two- to fivefold higher number of short mtDNA fragments in the nuclei of iPS cells compared to fibroblasts, large mtDNA fragments ($\sim$12 kb) were not enriched in the nuclei of iPS cells suggesting that large or even full-length mtDNA molecules are not amplified during reprogramming in the nuclei of iPS cells. We determined the sequences of the short mtDNA fragments (see Supplementary Fig. S4), which were amplified by PCR from MEF and iPS cell nuclear genomic DNA. All sequences of the amplified PCR fragments are identical to mtDNA sequences (Supplementary Sequence). We conclude that in the nuclei of iPS cells a high number of short mtDNA sequences are mainly present as extrachromosomal circles, although we cannot exclude that nuclear mtDNA insertions occur during reprogramming as well.

Like iPS cells, ES cells also exhibit culture-induced copy number variations in chromosomal DNA [53]. Therefore, we investigated whether mtDNA sequences with nuclear localization are present in elevated numbers in two different ES cell lines. We demonstrated that there was a significant increase (3.2-fold; $P < 0.005$) in nuclear mtDNA sequences in ES cells compared to fibroblast cells (Fig. 3 and Supplementary Fig. S5; Fig. 1B for quantification).

Given that the number of mtDNA sequences in the nucleus increases during reprogramming, we were interested in ascertaining whether these accumulated sequences remain at similar levels when the stem cells initiate differentiation into somatic cells. When we induced differentiation in pluripotent stem cells (iPS and ES cells) to somatic cells using the hanging drop method [47], the accumulated mtDNA species in nuclei of this heterogeneous population of differentiating cells decreased to similar levels as observed in fibroblasts (Fig. 4). Thus, the process of the accumulation of mtDNA sequences in nuclei is reversible.

In summary, we demonstrate that mtDNA sequences with nuclear localization are present in elevated numbers in both iPS and ES cells, but decreases when the pluripotent stem cells undergo differentiation to somatic cells. Most of the nuclear-amplified mtDNA sequences appear to be present in the extrachromosomal form. We envisage three possible mechanisms by which mtDNA enters into the nucleus and/or amplifies: (1) Fragmented mtDNA may translocate to the nucleus. If the mtDNA fragments enter the nucleus in the linear form they may either insert into the chromosomal DNA, which may occur during the repair of a dsDNA break in chromosomal DNA, or be converted to circular DNA molecules with the help of a DNA ligase (eg, Lig4 of the non-homologous end-joining pathway). (2) Alternatively, a few circles with mtDNA sequences may already be present in the nucleus and those may amplify during reprogramming. This is a likely possibility since in fibroblasts mtDNA sequences are already present in the nucleus (see Figs. 1 and 2), and some of these appear to be extrachromosomal (Fig. 2). Further support for this scenario comes from our observation, if mtDNA is removed from mitochondria using ethidium bromide, the accumulated mtDNA fragments still remain in about the similar amount in the nucleus suggesting that the translocation of mtDNA fragments to the nucleus appears rather not to be a requirement for the amplification of nuclear mtDNA fragments (Supplementary Fig. S6). The extrachromosomal mtDNA circles may be maintained and inherited in the nucleus by break-induced replication mechanisms [56,57]. (3) Another possible scenario is that a few single fibroblasts with already highly amplified mtDNA molecules in the nucleus may be the preferential source for the reprogramming to iPS cells.

The number and variety of extrachromosomal circular DNA in the nucleus increase enormously in tumor tissues and in cells exposed to carcinogens [58–61]. Overrepresentation of these circular DNAs may disturb chromosomal DNA replication and/or repair of damage in chromosomal DNA. A similar scenario might be linked to the amplification of mtDNA sequences in iPS cells. Expression of the reprogramming factors and oncogenes Klf4 and c-Myc may initiate the amplifications of mtDNA sequences in the nucleus and potentially contribute in this way to an increase in nuclear genomic instability. This is a possibility since deregulated c-Myc expression itself contributes to genomic instability, including the formation of extrachromosomal DNA circles [61].

Conclusions

We demonstrate in this study that pluripotent stem cells contain high numbers of mtDNA sequences in the nucleus, which decrease upon differentiation to somatic cells. This unexpected observation during reprogramming highlights a new feature of pluripotent stem cells, and may represent another level of chromosomal regulation. It is however unclear, whether high levels of mtDNA circles in the nucleus inhibit or improve reprogramming, which will be tested in future experiments.

Acknowledgments

We are grateful to Dr. Rudolf Jaenisch, Whitehead Institute, Cambridge, for providing the Oct4-GFP iPS cells,

Dr. Utz Herbig for providing the Cy3-labeled PNA telomere probe, Drs. Yanfei Yang and Junichi Sadoshima for providing GAPDH mouse DNA for labeling, Dr. Lin Yan for providing purified mitochondria derived from mouse hearts. We also thank Dr. Carolyn Suzuki for critical reading of the manuscript and Drs. Sadoshima, Toruner, Tyagi for discussions throughout the project. This work was supported by the NIH (J.S.S., D.F., and E.S.R.), the Muscular Dystrophy Association (D.F.), the Hispanic Center of Excellence (D.F.), and by departmental support (A.S.I. and D.F.).

Author Disclosure Statement

The authors indicate no potential conflict of financial interests.

References

1. Hazkani-Covo E, RM Zeller and W Martin. (2010). Molecular poltergeists: mitochondrial DNA copies (numts) in sequenced nuclear genomes. PLoS Genet 6:e1000834.
2. Thorsness PE and TD Fox. (1990). Escape of DNA from mitochondria to the nucleus in *Saccharomyces cerevisiae*. Nature 346:376–379.
3. Schiestl RH, M Dominska and TD Petes. (1993). Transformation of *Saccharomyces cerevisiae* with nonhomologous DNA: illegitimate integration of transforming DNA into yeast chromosomes and in vivo ligation of transforming DNA to mitochondrial DNA sequences. Mol Cell Biol 13:2697–2705.
4. Ricchetti M, C Fairhead and B Dujon. (1999). Mitochondrial DNA repairs double-strand breaks in yeast chromosomes. Nature 402:96–100.
5. Yu X and A Gabriel. (1999). Patching broken chromosomes with extranuclear cellular DNA. Mol Cell 4:873–881.
6. Decottignies A. (2005). Capture of extranuclear DNA at fission yeast double-strand breaks. Genetics 171:1535–1548.
7. Turner C, C Killoran, NS Thomas, M Rosenberg, NA Chuzhanova, J Johnston, Y Kemel, DN Cooper and LG Biesecker. (2003). Human genetic disease caused by de novo mitochondrial-nuclear DNA transfer. Hum Genet 112:303–309.
8. Ricchetti M, F Tekaia and B Dujon. (2004). Continued colonization of the human genome by mitochondrial DNA. PLoS Biol 2:E273.
9. Shay JW and H Werbin. (1992). New evidence for the insertion of mitochondrial DNA into the human genome: significance for cancer and aging. Mutat Res 275:227–235.
10. Goldin E, S Stahl, AM Cooney, CR Kaneski, S Gupta, RO Brady, JR Ellis and R Schiffmann. (2004). Transfer of a mitochondrial DNA fragment to MCOLN1 causes an inherited case of mucolipidosis IV. Hum Mutat 24:460–465.
11. Willett-Brozick JE, SA Savul, LE Richey and BE Baysal. (2001). Germ line insertion of mtDNA at the breakpoint junction of a reciprocal constitutional translocation. Hum Genet 109:216–223.
12. Borensztajn K, O Chafa, M Alhenc-Gelas, S Salha, A Reghis, AM Fischer and J Tapon-Bretaudiere. (2002). Characterization of two novel splice site mutations in human factor VII gene causing severe plasma factor VII deficiency and bleeding diathesis. Br J Haematol 117:168–171.
13. Liang BC. (1996). Evidence for association of mitochondrial DNA sequence amplification and nuclear localization in human low-grade gliomas. Mutat Res 354:27–33.
14. Chen D, W Xue and J Xiang. (2008). The intra-nucleus integration of mitochondrial DNA (mtDNA)in cervical mucosa cells and its relation with c-myc expression. J Exp Clin Cancer Res 27:36.
15. Cheng X and AS Ivessa. (2010). The migration of mitochondrial DNA fragments to the nucleus affects the chronological aging process of *Saccharomyces cerevisiae*. Aging Cell 89:742–747.
16. Cheng X and AS Ivessa. (2012). Accumulation of linear mitochondrial DNA fragments in the nucleus shortens the chronological life span of yeast. Eur J Cell Biol 91:782–788.
17. Caro P, J Gomez, A Arduini, M Gonzalez-Sanchez, M Gonzalez-Garcia, C Borras, J Vina, MJ Puertas, J Sastre and G Barja. (2010). Mitochondrial DNA sequences are present inside nuclear DNA in rat tissues and increase with age. Mitochondrion 10:479–486.
18. Takahashi K, K Tanabe, M Ohnuki, M Narita, T Ichisaka, K Tomoda and S Yamanaka. (2007). Induction of pluripotent stem cells from adult human fibroblasts by defined factors. Cell 131:861–872.
19. Takahashi K and S Yamanaka. (2006). Induction of pluripotent stem cells from mouse embryonic and adult fibroblast cultures by defined factors. Cell 126:663–676.
20. Plath K and WE Lowry. (2011). Progress in understanding reprogramming to the induced pluripotent state. Nat Rev Genet 12:253–265.
21. Robinton DA and GQ Daley. (2012). The promise of induced pluripotent stem cells in research and therapy. Nature 481:295–305.
22. Morris SA and GQ Daley. (2013). A blueprint for engineering cell fate: current technologies to reprogram cell identity. Cell Res 23:33–48.
23. Rais Y, A Zviran, S Geula, O Gafni, E Chomsky, S Viukov, AA Mansour, I Caspi, V Krupalnik, et al. (2013). Deterministic direct reprogramming of somatic cells to pluripotency. Nature 502:65–70.
24. Blasco MA, M Serrano and O Fernandez-Capetillo. (2011). Genomic instability in iPS: time for a break. EMBO J 30: 991–993.
25. Marion RM, K Strati, H Li, M Murga, R Blanco, S Ortega, O Fernandez-Capetillo, M Serrano and MA Blasco. (2009). A p53-mediated DNA damage response limits reprogramming to ensure iPS cell genomic integrity. Nature 460:1149–1153.
26. Hussein SM, NN Batada, S Vuoristo, RW Ching, R Autio, E Narva, S Ng, M Sourour, R Hamalainen, et al. (2011). Copy number variation and selection during reprogramming to pluripotency. Nature 471:58–62.
27. Gore A, Z Li, HL Fung, JE Young, S Agarwal, J Antosiewicz-Bourget, I Canto, A Giorgetti, MA Israel, et al. (2011). Somatic coding mutations in human induced pluripotent stem cells. Nature 471:63–67.
28. Pasi CE, A Dereli-Oz, S Negrini, M Friedli, G Fragola, A Lombardo, G Van Houwe, L Naldini, S Casola, et al. (2011). Genomic instability in induced stem cells. Cell Death Differ 18:745–753.
29. Mayshar Y, U Ben-David, N Lavon, JC Biancotti, B Yakir, AT Clark, K Plath, WE Lowry and N Benvenisty. (2010). Identification and classification of chromosomal aberrations in human induced pluripotent stem cells. Cell Stem Cell 7:521–531.
30. Taapken SM, BS Nisler, MA Newton, TL Sampsell-Barron, KA Leonhard, EM McIntire and KD Montgomery. (2011). Karotypic abnormalities in human induced pluripotent stem cells and embryonic stem cells. Nat Biotechnol 29:313–314.
31. Wissing S, M Munoz-Lopez, A Macia, Z Yang, M Montano, W Collins, JL Garcia-Perez, JV Moran and WC Greene.

(2012). Reprogramming somatic cells into iPS cells activates LINE-1 retroelement mobility. Hum Mol Genet 21:208–218.
32. Ronen D and N Benvenisty. (2012). Genomic stability in reprogramming. Curr Opin Genet Dev 22:444–449.
33. Hong SG, CE Dunbar and T Winkler. (2012). Assessing the risks of genotoxicity in the therapeutic development of induced pluripotent stem cells. Mol Ther 21:272–281.
34. Luo LZ, S Gopalakrishna-Pillai, SL Nay, SW Park, SE Bates, X Zeng, LE Iverson and TR O'Connor. (2012). DNA repair in human pluripotent stem cells is distinct from that in non-pluripotent human cells. PLoS One 7:e30541.
35. Momcilovic O, L Knobloch, J Fornsaglio, S Varum, C Easley and G Schatten. (2010). DNA damage responses in human induced pluripotent stem cells and embryonic stem cells. PLoS One 5:e13410.
36. Deng W and Y Xu. (2009). Genome integrity: linking pluripotency and tumorgenicity. Trends Genet 25:425–427.
37. Martins-Taylor K, BS Nisler, SM Taapken, T Compton, L Crandall, KD Montgomery, M Lalande and RH Xu. (2011). Recurrent copy number variations in human induced pluripotent stem cells. Nat Biotechnol 29:488–491.
38. Laurent LC, I Ulitsky, I Slavin, H Tran, A Schork, R Morey, C Lynch, JV Harness, S Lee, et al. (2011). Dynamic changes in the copy number of pluripotency and cell proliferation genes in human ESCs and iPSCs during reprogramming and time in culture. Cell Stem Cell 8:106–118.
39. Ji J, SH Ng, V Sharma, D Neculai, S Hussein, M Sam, Q Trinh, GM Church, JD McPherson, A Nagy and NN Batada. (2012). Elevated coding mutation rate during the reprogramming of human somatic cells into induced pluripotent stem cells. Stem Cells 30:435–440.
40. Young MA, DE Larson, CW Sun, DR George, L Ding, CA Miller, L Lin, KM Pawlik, K Chen, et al. (2012). Background mutations in parental cells account for most of the genetic heterogeneity of induced pluripotent stem cells. Cell Stem Cell 10:570–582.
41. Quinlan AR, MJ Boland, ML Leibowitz, S Shumilina, SM Pehrson, KK Baldwin and IM Hall. (2011). Genome sequencing of mouse induced pluripotent stem cells reveals retroelement stability and infrequent DNA rearrangement during reprogramming. Cell Stem Cell 9:366–373.
42. Kuttler F and S Mai. (2006). c-Myc, genomic instability and disease. Genome Dyn 1:171–190.
43. Marzi I, MG Cipolleschi, M D'Amico, T Stivarou, E Rovida, MC Vinci, S Pandolfi, P Dello Sbarba, B Stecca and M Olivotto. (2013). The involvement of a Nanog, Klf4 and c-Myc transcriptional circuitry in the intertwining between neoplastic progression and reprogramming. Cell Cycle 12:353–364.
44. Chang CW, YS Lai, KM Pawlik, K Liu, CW Sun, C Li, TR Schoeb and TM Townes. (2009). Polycistronic lentiviral vector for ''hit and run'' reprogramming of adult skin fibroblasts to induced pluripotent stem cells. Stem Cells 27:1042–1049.
45. Meissner A, M Wernig and R Jaenisch. (2007). Direct reprogramming of genetically unmodified fibroblasts into pluripotent stem cells. Nat Biotechnol 25:1177–1181.
46. Friedrich G and P Soriano. (1991). Promoter traps in embryonic stem cells: a genetic screen to identify and mutate developmental genes in mice. Genes Dev 5:1513–1523.
47. Lupu F, A Alves, K Anderson, V Doye and E Lacy. (2008). Nuclear pore composition regulates neural stem/progenitor cell differentiation in the mouse embryo. Dev Cell 14: 831–842.
48. King MP and G Attardi. (1996). Isolation of human cell lines lacking mitochondrial DNA. Methods Enzymol 264:304–313.
49. Kolesar JE, CY Wang, YV Taguchi, SH Chou and BA Kaufman. (2013). Two-dimensional intact mitochondrial DNA agarose electrophoresis reveals the structural complexity of the mammalian mitochondrial genome. Nucleic Acids Res 41:e58.
50. Hande MP, AS Balajee, A Tchirkov, A Wynshaw-Boris and PM Lansdorp. (2001). Extra-chromosomal telomeric DNA in cells from Atm(-/-) mice and patients with ataxia-telangiectasia. Hum Mol Genet 10:519–528.
51. Ivessa AS, J-Q Zhou and VA Zakian. (2000). The *Saccharomyces* Pif1p DNA helicase and the highly related Rrm3p have opposite effects on replication fork progression in ribosomal DNA. Cell 100:479–489.
52. Takahashi K, K Okita, M Nakagawa and S Yamanaka. (2007). Induction of pluripotent stem cells from fibroblast cultures. Nat Protoc 2:3081–3089.
53. Narva E, R Autio, N Rahkonen, L Kong, N Harrison, D Kitsberg, L Borghese, J Itskovitz-Eldor, O Rasool, et al. (2010). High-resolution DNA analysis of human embryonic stem cell lines reveals culture-induced copy number changes and loss of heterozygosity. Nat Biotechnol 28:371–377.
54. Geimanen J, H Isok-Paas, R Pipitch, K Salk, T Laos, M Orav, T Reinson, M Ustav, Jr., M Ustav and E Ustav. (2011). Development of a cellular assay system to study the genome replication of high- and low-risk mucosal and cutaneous human papillomaviruses. J Virol 85:3315–3329.
55. Martinez-Robles ML, G Witz, P Hernandez, JB Schvartzman, A Stasiak and DB Krimer. (2009). Interplay of DNA supercoiling and catenation during the segregation of sister duplexes. Nucleic Acids Res 37:5126–5137.
56. Costantino L, SK Sotiriou, JK Rantala, S Magin, E Mladenov, T Helleday, JE Haber, G Iliakis, OP Kallioniemi and TD Halazonetis. (2014). Break-induced replication repair of damaged forks induces genomic duplications in human cells. Science 343:88–91.
57. Sakofsky CJ, S Ayyar and A Malkova. (2012). Break-induced replication and genome stability. Biomolecules 2:483–504.
58. Cohen S and S Lavi. (1996). Induction of circles of heterogeneous sizes in carcinogen-treated cells: two-dimensional gel analysis of circular DNA molecules. Mol Cell Biol 16: 2002–2014.
59. Cohen Z, E Bacharach and S Lavi. (2006). Mouse major satellite DNA is prone to eccDNA formation via DNA Ligase IV-dependent pathway. Oncogene 25:4515–4524.
60. Cohen S, A Regev and S Lavi. (1997). Small polydispersed circular DNA (spcDNA) in human cells: association with genomic instability. Oncogene 14:977–985.
61. Kuttler F and S Mai. (2007). Formation of non-random extrachromosomal elements during development, differentiation and oncogenesis. Semin Cancer Biol 17:56–64.

Address correspondence to:
Andreas S. Ivessa
Department of Cell Biology and Molecular Medicine
Rutgers New Jersey Medical School
Rutgers Biomedical and Health Sciences
185 South Orange Avenue
Newark, NJ 07101-1709

E-mail: ivessaan@njms.rutgers.edu

Received for publication December 19, 2013
Accepted after revision June 20, 2014
Prepublished on Liebert Instant Online June 25, 2014